

Universal scaling of correlated diffusion of colloidal particles near a liquid-liquid interface

Cite as: Appl. Phys. Lett. **103**, 154102 (2013); <https://doi.org/10.1063/1.4824653>

Submitted: 14 August 2013 . Accepted: 22 September 2013 . Published Online: 11 October 2013

Wei Zhang, Song Chen, Na Li, Jiazheng Zhang, and Wei Chen



View Online



Export Citation



CrossMark

ARTICLES YOU MAY BE INTERESTED IN

[Structure and dynamics of a layer of sedimented particles](#)

The Journal of Chemical Physics **143**, 074704 (2015); <https://doi.org/10.1063/1.4928644>

[Anisotropic diffusion of concentrated hard-sphere colloids near a hard wall studied by evanescent wave dynamic light scattering](#)

The Journal of Chemical Physics **139**, 164905 (2013); <https://doi.org/10.1063/1.4825261>

[Motion of a spherical particle near a planar fluid-fluid interface: The effect of surface incompressibility](#)

The Journal of Chemical Physics **133**, 114702 (2010); <https://doi.org/10.1063/1.3475197>

Lock-in Amplifiers up to 600 MHz

starting at

\$6,210



Zurich Instruments

Watch the Video



AIP
Publishing

Universal scaling of correlated diffusion of colloidal particles near a liquid-liquid interface

Wei Zhang,^{1,2,a)} Song Chen,¹ Na Li,¹ Jiazheng Zhang,¹ and Wei Chen^{1,a)}

¹State Key Laboratory of Surface Physics, Department of Physics, Fudan University, Shanghai, China

²Department of Physics, Jinan University, Guangzhou, China

(Received 14 August 2013; accepted 22 September 2013; published online 11 October 2013)

In this letter, we investigate the correlated diffusion of colloidal particles in quasi two-dimensional monolayer near an oil-water interface for different distance between the interface and the particle monolayer z . It is found that there is a transition in the behavior of the correlated diffusion from the bulk dominated to the interface dominated with decreasing z or increasing inter-particle separation r . With a scaling method proposed by us, the correlated diffusion can be scaled onto a master curve which captures the characters of this transition. The scale factors and the master curve allow the calculation of the distance z , which are in agreement with the one-particle measurements. © 2013 AIP Publishing LLC. [<http://dx.doi.org/10.1063/1.4824653>]

The dynamic behavior of confined colloidal suspensions has attracted a lot of attention in recent years.^{1–6} In real circumstances, particles are usually spatially confined in special environments, such as microfluidic devices, porous media, fluid interface, or cell membrane.^{7–13} Compared with unbounded three-dimensional (3D) fluid bulk, colloid behavior in spatially confined environments is more complicated. In unbounded 3D bulk suspensions, the longitudinal and transverse correlated diffusion coefficients D_{\parallel} and D_{\perp} are well known as $D_{\parallel}, D_{\perp} \propto 1/r$ and $D_{\parallel} = 2D_{\perp}$,¹⁴ where r is the inter-particle distance. For particles confined by the solid wall, the strength of the hydrodynamic interactions (HIs) decay with r as $1/r^2$.^{4,15,16} The breaking in the spatial symmetry due to the boundary conditions introduces asymmetry to the correlated diffusion of particles. Such as particles at an air-water interface or a viscous membrane, both theoretical¹⁷ and experimental¹⁸ studies show $D_{\parallel} \propto 1/r$ and $D_{\perp} \propto 1/r^2$. When there is a solid wall adjacent to a membrane, Oppenheimer and Diamant¹⁹ demonstrated that the correlated diffusion of particles at the membrane is also a function of the distance between the membrane and the solid wall.

The influence of different boundary conditions could be directly reflected in the diffusion behavior of particles.^{20–24} Many studies have focused on solid-wall conditions with a non-slip boundary, which could cut off the fluid field in its vicinity. For a fluid-fluid interface (say, a soft wall), there is a slip boundary that partially transforms the surrounding flow field. Despite extensive investigations on the effects of the solid wall, there are comparatively few experimental studies on the influences of the fluid-fluid interface on the correlated diffusion of particles.

In this letter, we report an experimental measurement of the correlated diffusion of colloidal particles near a water-decahydronaphthalene (decalin) interface. It is shown that the effects of the interface on the longitudinal and transverse correlated diffusion are different. With decreasing the distance between the particles and the interface z or increasing r , there is a transition of the correlated diffusion behavior

from the 3D bulk to the interface dominated. We propose a scaling method with which the correlated diffusion of particles in colloidal monolayer with different z can be scaled onto a master curve that characterizes this transition. The scaling factor and the master curve could be used to calculate the distance z . The obtained results are of significance for understanding the dynamical behaviors of particles near the liquid-liquid interface and may be helpful for soft-wall's applications.

Three kinds of samples of uniform colloidal particles were used: polystyrene (PS) latex spheres with a diameter $d = 2.0 \mu\text{m}$ and silica spheres with a diameter $d = 2.0 \mu\text{m}$ (S1) and $d = 1.57 \mu\text{m}$ (S2). The PS spheres with sulfate group were purchased from Invitrogen, and the silica spheres were purchased from Bangs. These silica spheres acquire anionic SiO^- groups on their surfaces when they are dispersed in water. Both the PS and silica spheres are representative of the charged particles that are commonly used in colloidal science. The PS and silica samples are suspended in deionized water of $18.2 \text{ M}\Omega \cdot \text{cm}$ and are cleaned seven times by centrifugation to eliminate any possible surfactant before use.

The experimental setup is similar to that in Ref. 25. The sample cell is composed of a stainless steel disk with an inner container in which there is a hole of the diameter 8.3 mm, and the bottom of this hole is sealed with a 0.1 mm thick glass cover slip, that also serves as an optical window. First, we fill the hole with the cleaned water-sphere suspension, and then we add decalin (a mixture of cis and trans with a density of 0.896 g/cm^3) purchased from Sigma-Aldrich to the top of the suspension, completely filling the inner container. Another cover slip is used to cover the top of the inner container, then, we flip the cell over quickly, and let it settle upside-down for two hours. The water layer could remain on the top, and the oil stay on the bottom and will not rise up, because the fluids are completely pinned by the surrounding solid boundaries. Due to gravity, particles fall onto the water-decalin interface and form a monolayer, as shown in Fig. 1. The colloidal particles are hydrophilic and preferentially remain in the water rather than sinking into decalin. In addition, particle's image charge in decalin has same sign as the surface charge of the particles, because these particles

^{a)}Authors to whom correspondence should be addressed. Electronic addresses: wzhangph@gmail.com and phchenwei@fudan.edu.cn

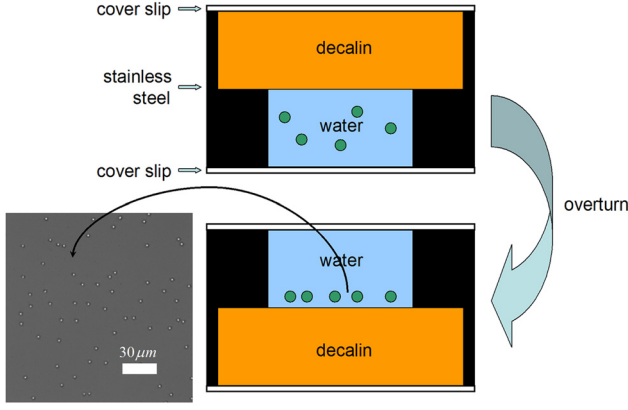


FIG. 1. A schematic of the process of the sample preparation and an optical microscope image of the silica spheres ($d = 2.0 \mu\text{m}$) suspended near the water-decalin interface at an area fraction of $n = 0.01$.

remain in the medium (water) with the higher dielectric constant.²⁶ The Coulomb repulsion keeps particles a certain distance away from the interface. The water and decalin layers are both 0.8 mm thick, and the distance between the cover slip and the colloidal monolayer is sufficiently large to eliminate the any potential influence from cover slips. Using an inverted Olympus IX71 microscope, the motion of the colloidal particles was recorded by a digital camera (Prosilica GE1050) at a rate of 14 frames per second. Each image sequence includes 500 consecutive frames and each image is $176 \times 176 \mu\text{m}^2$. Using a homemade software, we obtain the particle positions from these image sequences and construct their trajectories.

Particle's motion normal to the interface is very weak. We focus our investigation on the lateral motion of the particles, i.e., their motion parallel to the oil-water interface, in the following part of the letter. The distance from particle center to the interface depends on the mass density and surface charge of colloidal particles. The average distance from the particle monolayer to the interface, z , can be estimated by measuring the self-diffusion coefficient of the particles, which is referred to as one-particle measurements. From the particle trajectories $\mathbf{s}(t)$, we calculate the one-particle mean square displacement (MSD) $\langle \Delta \mathbf{s}^2(\tau) \rangle = \langle |\mathbf{s}(t + \tau) - \mathbf{s}(t)|^2 \rangle$. The self-diffusion coefficient D_s is obtained according to the equation $\langle \Delta \mathbf{s}^2(\tau) \rangle = 4D_s\tau$ for different particle area fractions n . Figure 2 shows the dependence of the diffusion coefficient D_s/D_0 on n for the PS and S1 spheres, where $D_0 = k_B T / 3\pi\eta_w d$ is the diffusion coefficient of a single particle in water. The solid lines in Fig. 2 shows the second-order polynomial fitted results

$$D_s/D_0 = \alpha(1 - \beta n - \gamma n^2). \quad (1)$$

The parameter α represents the local viscosity experienced by a single sphere at the dilute limit: a larger α implies a smaller viscosity. The parameter β reflects the strength of the two-body HIs between two spheres: a smaller β implies a smaller two-body HIs. The fitted values of α , β , and γ are given in Table I.

The value of α can be used to estimate the distance between the interface and the particle monolayer, z_{1p} , where the subscript $1p$ refers to one-particle measurements.

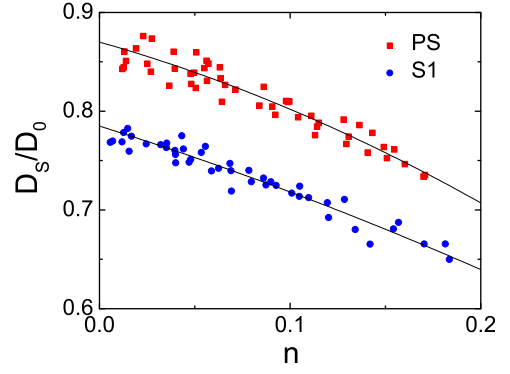


FIG. 2. The measured self-diffusion coefficient D_s scaled by D_0 as a function of the particle area fraction n . Different symbols represent data for different particles. The solid lines show the second-order polynomial fitting $D_s/D_0 = \alpha(1 - \beta n - \gamma n^2)$.

According to the classical prediction given by Lee *et al.*^{24,27} the distance from a particle's center to the interface can be written as

$$z_{1p} = \frac{3d(2\eta_w - 3\eta_o)}{32(\eta_w + \eta_o)(\alpha - 1)}, \quad (2)$$

where η_w is the viscosity of water and $\eta_o = 2.5 \text{ cP}$ is the viscosity of decalin at 22.5 °C. By substituting the fitted values of α into Eq. (2), we obtain $z_{1p} = 2.3 \pm 0.2 \mu\text{m}$ for PS spheres and $1.4 \pm 0.1 \mu\text{m}$ for S1 spheres. This calculation is consistent with the microscope observation, which demonstrated that the particles remain at a distance of $1 - 2 \mu\text{m}$ from the interface.

By tracking the trajectory $\mathbf{s}^i(t)$ of an individual particle i , the particle's cross-correlated motion is obtained via the ensemble-averaged tensor products of the particle's displacements¹⁴

$$M_{xy}(\Upsilon, \tau) = \langle \Delta s_x^i(t, \tau) \Delta s_y^j(t, \tau) \delta(\Upsilon - r^{ij}(t)) \rangle_{i \neq j, t}. \quad (3)$$

Here $\Delta s_x^i(t, \tau) = s_x^i(t + \tau) - s_x^i(t)$. In the above equation, i and j indicate distinct particle, x and y represent different coordinates, and r^{ij} is the separation between particles i and j . Because the off-diagonal elements are uncorrelated, we focus on the diagonal elements of this tensor product, namely, M_{rr} which indicates the correlated motion along the line connecting the centers of the particles, and $M_{\theta\theta}$ which represents the correlated motion perpendicular to this line. We found that the measured correlated motions, M_{rr} and $M_{\theta\theta}$, are linear functions of τ for a small time lag τ . Thus, the longitudinal and transverse correlated diffusion coefficients are defined as $D_{||} = M_{rr}/2\tau$ and $D_{\perp} = M_{\theta\theta}/2\tau$.

TABLE I. The measured one-particle distance from colloidal monolayer to the interface z_{1p} and the fitted values of the second-order polynomial fitting $D_s/D_0 = \alpha(1 - \beta n - \gamma n^2)$ for different colloidal spheres.

Sample	z_{1p} (μm)	α	β	γ
PS	2.3 ± 0.2	0.87 ± 0.01	0.62 ± 0.12	1.54 ± 0.61
S1	1.4 ± 0.1	0.78 ± 0.01	0.78 ± 0.02	0.76 ± 0.03
S2	1.4 ± 0.1	0.83 ± 0.01	0.80 ± 0.08	1.43 ± 0.04

Figure 3(a) exhibits $D_{\parallel}/\alpha D_0$ and $D_{\perp}/\alpha D_0$ of the PS and S1 spheres as a function of r/d . Each curve was obtained by averaging at least 10^6 particle positions. The behaviors of $D_{\parallel}/\alpha D_0$ and $D_{\perp}/\alpha D_0$ of the PS and S1 monolayers are qualitatively similar. With the increase of the inter-particle separation r , $D_{\parallel}/\alpha D_0$ and $D_{\perp}/\alpha D_0$ of the PS and S1 spheres decrease in the form of power law. In the parallel direction, the experimental results show that $D_{\parallel}(r)/\alpha D_0 = C_{\parallel}r^{-k_{\parallel}}$. Here, C_{\parallel} is the amplitude coefficient and $k_{\parallel} = 1$ is the decay rate of the correlated motion. The interface distance z affects the amplitude C_{\parallel} but not the decay rate k_{\parallel} . The amplitude C_{\parallel} of the S1 spheres is larger than that of the PS spheres, which is in accordance with the single-diffusion measurements: the fitted value β of the S1 spheres is greater than that of the PS spheres, as displayed in Table I. The fact that the same decay rate $k_{\parallel} = 1$ was observed for both monolayers indicates that the interface has little effect on the form of HIs in the parallel direction.

In the perpendicular direction, $D_{\perp}(r)/\alpha D_0 = C_{\perp}r^{-k_{\perp}}$. Both the amplitude C_{\perp} and the decay rate k_{\perp} are functions of the distance z . The decay rate k_{\perp} of the S1 spheres is larger than that of the PS spheres for small r . The decay rate k_{\perp} increases with increasing r . For a large r , k_{\perp} for both the PS monolayer and the S1 monolayer converges to approximately 2, as shown in Fig. 3(a).

The cross correlated motion of colloidal spheres near an oil-water interface is similar to that at a viscous membrane:^{17,18} $k_{\parallel} = 1$ and $k_{\perp} = 2$ when $r \gg z$. For small r , the value of k_{\perp} for the S1 spheres is larger than that of the PS spheres stems from the HIs that are modified by the

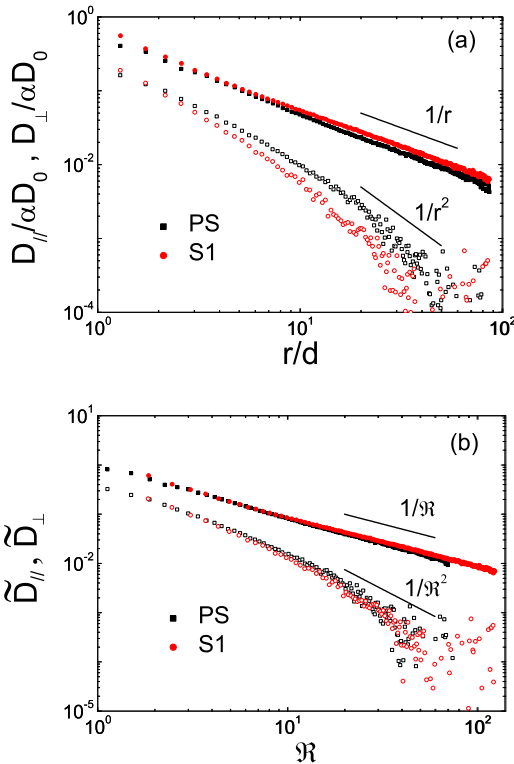


FIG. 3. (a) The measured correlated diffusion coefficient $D_{\parallel}/\alpha D_0$ (solid symbols) and $D_{\perp}/\alpha D_0$ (open symbols) as a function of the scaled inter-particle distance r/d for the PS and S1 spheres. (b) Master curve of scaled correlated diffusion coefficient \tilde{D}_{\parallel} (solid symbols) and \tilde{D}_{\perp} (open symbols) as a function of the scaled distance $\mathfrak{R} = r/z$. The used scaling parameter z is from Table I. Symbols are the same as those in (a). The solid lines with slopes -1 and -2 are visual guides.

interface. Because the oil is more viscous than water, the flow field induced by the particles in water is suppressed by the oil-water interface. In addition, the HIs between particles at a distance r decay rapidly when the monolayer is closer to the interface, which leads to a larger measured k_{\perp} for a smaller z .

Analogous to the correlated motion of the particles at a viscous membrane with various surface viscosity,¹⁸ D_{\parallel} and D_{\perp} for different z can also be scaled onto a single master curve. We define dimensionless correlated diffusion functions $\tilde{D}_{\parallel,\perp} = D_{\parallel,\perp}/D_e$, where $D_e = k_B T / (6\pi\eta_w z)$, and a scaled separation $\mathfrak{R} = r/z$. The values of the scaling parameter D_e and z for the PS and S1 spheres are obtained from Eq. (2). Figure 3(b) shows the scaled correlated diffusion coefficients \tilde{D}_{\parallel} and \tilde{D}_{\perp} as a function of the scaled separation \mathfrak{R} for the PS and S1 spheres. As shown in Fig. 3(b), the data of particles with different z fall on a single master curve. At small \mathfrak{R} region ($\mathfrak{R} \lesssim 1.5$), $\tilde{D}_{\parallel}, \tilde{D}_{\perp} \propto 1/\mathfrak{R}$, which is the characteristics of the 3D bulk.¹⁴ At large \mathfrak{R} region ($\mathfrak{R} \gtrsim 20$), $\tilde{D}_{\parallel} \propto 1/\mathfrak{R}$, $\tilde{D}_{\perp} \propto 1/\mathfrak{R}^2$, which is the characteristics of the two-dimensional interface.^{17,18} At the intermediate region of \mathfrak{R} , \tilde{D}_{\perp} shows a crossover behavior.

Using the scale factors and the master curve, one could measure the distance between the particles and the interface z . We know that both scaling parameters D_e and z are only the function of the distance z . We allow $\tilde{D}_{\parallel}(\mathfrak{R})$ and $\tilde{D}_{\perp}(\mathfrak{R})$ of the S2 spheres to fall on the master curve in Fig. 3(b) to obtain the measurement of the distance between the particles and the interface z_{2p} , as shown in Fig. 4. Here the subscript $2p$ indicates two-particle measurement. The correlated diffusion coefficients before scaling of the S2 spheres are exhibited in the inset of Fig. 4. The measured distance z_{2p} for the S2 spheres is equal to $1.4 \pm 0.1 \mu\text{m}$ which is in agreement with the one-particle measurement result z_{1p} shown in Table I.

The distance z includes the information of particle size and fluid viscosity. By moving the correlated diffusion curve onto the master curve, one could measure the distance z without particle size information. The experimental results show that the analytical equation of the master curve can be written

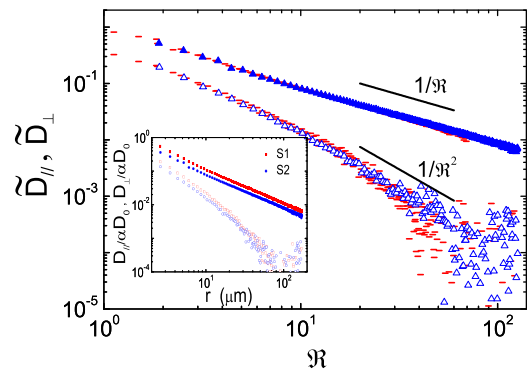


FIG. 4. The scaled correlated diffusion coefficient \tilde{D}_{\parallel} (solid symbols) and \tilde{D}_{\perp} (open symbols) as a function of the scaled distance $\mathfrak{R} = r/z$ for the S2 spheres. The dashed line is the master curve showed in Fig. 3(b). The measured two-particle distance $z_{2p} = 1.4 \pm 0.1 \mu\text{m}$ is in agreement with the one-particle measurements. The solid lines with slopes -1 and -2 are visual guides. The inset exhibits the measured correlated diffusion coefficient $D_{\parallel}/\alpha D_0$ (solid symbols) and $D_{\perp}/\alpha D_0$ (open symbols) as a function of the inter-particle separation r for the S1 and S2 spheres.

as the form: $D_{\parallel,\perp}/D_e = f_{\parallel,\perp}(r/z)$. At present, we could not present the specific expression of the function f theoretically, which deserves further theoretical investigation.

The data in Figs. 3 and 4 measured were in the area fraction range $n < 0.2$. For particles in a plane near an oil-water interface, the density has no effects on D_{\parallel} and D_{\perp} for the momentum propagation between particles is mainly through the surrounding fluid rather than the particle monolayer in the area fraction range we measured. The HIs through particle monolayer contribute to the correlated motion only when the separation r is less than the order of Saffman-Delbruck length $L_s = \eta_m/(\eta_o + \eta_w)$.²⁸ In our system, the viscosity η_m of the monolayer is very small, and we have not measured the n effect. This n independence effect of the correlated diffusion coefficient is similar to that for particles confined between two plates measured by Cui *et al.*¹⁵ Thus, the scaling scheme presented in the letter still works when the system leaves the dilute limit.

In conclusion, the present work demonstrates that the oil-water interface influences the correlated diffusion of colloidal particles in longitudinal and transverse direction in different ways. Along the line connecting the centers of a pair of particles, the interface enhances the amplitude of the correlated diffusion coefficient D_{\parallel} , but does not affect its decay rate. In the direction perpendicular to this line, however, the decay rate of D_{\perp} increases with decreasing the distance between colloidal monolayer and the interface z for short inter-particle separation r . After scaling $D_{\parallel,\perp}$ and r with D_e and z , respectively, the correlated diffusion coefficients of particles with different z can fall on a single master curve. With the scaling parameter and the master curve, one could obtain the distance z which agrees well with the one-particle measurements. The master curve shows a crossover behavior in the intermediate region of \mathfrak{R} , which may be useful for clear understanding the dynamical behaviors of particles from high- to low-dimension.

We are grateful to Penger Tong from HKUST for helpful discussions. This work was supported in part by the

National Science Fund for Talent Training in Basic Science (Grant No. J1103204).

- ¹H. S. Binks and T. S. Horozov, *Colloidal Particles at Liquid Interfaces* (Cambridge University Press, Cambridge, 2006).
- ²E. R. Dufresne, T. M. Squires, M. P. Brenner, and D. G. Grier, *Phys. Rev. Lett.* **85**, 3317 (2000).
- ³B. Lin, J. Yu, and S. A. Rice, *Phys. Rev. E* **62**, 3909 (2000).
- ⁴P. L. Pushkar, W. S. James, F. B. John, J. W. Norman, and M. F. Eric, *Soft Matter* **7**, 6844 (2011).
- ⁵A. J. Levine and F. C. MacKintosh, *Phys. Rev. E* **66**, 061606 (2002).
- ⁶G. M. Wang, R. Prabhakar, Y. X. Gao, and E. M. Sevick, *J. Opt.* **13**, 044009 (2011).
- ⁷G. M. Whitesides and A. D. Stroock, *Phys. Today* **54**(6), 42 (2001).
- ⁸M. Sickert and F. Rondelez, *Phys. Rev. Lett.* **90**, 126104 (2003).
- ⁹J. Wu and L. L. Dai, *Appl. Phys. Lett.* **89**, 094107 (2006).
- ¹⁰F. Ortega, H. Ritacco, and R. G. Rubio, *Curr. Opin. Colloid Interface Sci.* **15**, 237 (2010).
- ¹¹W. Chen, S. Tan, T. K. Ng, W. T. Ford, and P. Tong, *Phys. Rev. Lett.* **95**, 218301 (2005).
- ¹²C. Wu, Y. Song, and L. L. Dai, *Appl. Phys. Lett.* **95**, 144104 (2009).
- ¹³A. Pralle, P. Keller, E.-L. Florin, K. Simons, and J. K. H. Hoirber, *J. Cell Biol.* **148**, 997 (2000).
- ¹⁴J. C. Crocker, M. T. Valentine, Eric R. Weeks, T. Gisler, P. D. Kaplan, A. G. Yodh, and D. A. Weitz, *Phys. Rev. Lett.* **85**, 888 (2000).
- ¹⁵B. Cui, H. Diamant, and B. Lin, *Phys. Rev. Lett.* **92**, 258301 (2004).
- ¹⁶H. Diamant, B. Cui, B. Lin, and S. A. Rice, *J. Phys.: Condens. Matter* **17**, S2787 (2005); **17**, S4047 (2005).
- ¹⁷N. Oppenheimer and H. Diamant, *Biophys. J.* **96**, 3041 (2009).
- ¹⁸V. Prasad, S. A. Koehler, and Eric R. Weeks, *Phys. Rev. Lett.* **97**, 176001 (2006).
- ¹⁹N. Oppenheimer and H. Diamant, *Phys. Rev. E* **82**, 041912 (2010).
- ²⁰G. S. Perkins and R. B. Jones, *Physica A* **171**, 575 (1991); **189**, 447 (1992).
- ²¹T. Bickel, *Phys. Rev. E* **75**, 041403 (2007).
- ²²B. Cichocki, M. L. Ekiel-Jezewska, and E. Wajnryb, *J. Chem. Phys.* **126**, 184704 (2007).
- ²³J. Blawdziewicz, M. L. Ekiel-Jezewska, and E. Wajnryb, *J. Chem. Phys.* **133**, 114703 (2010).
- ²⁴S. H. Lee, R. S. Chadwick, and L. G. Leal, *J. Fluid Mech.* **93**, 705 (1979).
- ²⁵Y. Peng, W. Chen, T. M. Fischer, D. A. Weitz, and P. Tong, *J. Fluid Mech.* **618**, 243 (2009).
- ²⁶E. C. Mbamala and H. H. von Grunberg, *J. Phys.: Condens. Matter* **14**, 4881 (2002).
- ²⁷G. M. Wang, R. Prabhakar, and E. M. Sevick, *Phys. Rev. Lett.* **103**, 248303 (2009).
- ²⁸P. G. Saffman and M. Delbruck, *Proc. Natl. Acad. U.S.A.* **72**, 3111 (1975).